Article

Optimization of Pea Protein Isolate-Stabilized Oil-in-Water Ultra-Nanoemulsions by Response Surface Methodology and the Effect of Electrolytes on Optimized Nanoemulsions

Anuj Niroula [†] [ID], Rodah Alshamsi [†], Bhawna Sobti * and Akmal Nazir *

Department of Food Science, College of Agriculture and Veterinary Medicine, United Arab Emirates University, Al Ain 15551, United Arab Emirates
* Correspondence: bhawna.chugh@uaeu.ac.ae (B.S.); akmal.nazir@uaeu.ac.ae (A.N.)
† These authors contributed equally to this work.

Abstract: Nanoemulsions are optically transparent and offer good stability, bioavailability, and control over the targeted delivery and release of lipophilic active components. In this study, pea protein isolate (PPI)-stabilized O/W nanoemulsions were evaluated using response surface methodology to obtain optimized ultra-nanoemulsions of Sauter mean diameter ($D_{3,2}$) < 100 nm using a high-pressure homogenizer (HPH). Furthermore, the effect of food matrix electrolytes, i.e., the pH and ionic strength, on the emulsion (prepared at optimized conditions) was investigated. The results revealed that the droplet size distribution of emulsions was mainly influenced by the PPI concentration and the interaction of oil concentration and HPH pressure. Moreover, a non-significant increase in droplet size was observed when the nanoemulsions (having an initial $D_{3,2}$ < 100 nm) were stored at 4 °C for 7 days. Based on the current experimental design, nanoemulsions with a droplet size < 100 nm can effectively be prepared with a high PPI concentration (6.35%), with less oil (1.95%), and at high HPH pressure (46.82 MPa). Such emulsions were capable of maintaining a droplet size below 100 nm even at ionic conditions of up to 400 mM NaCl and at acidic pH.

Keywords: Pickering emulsion; nanoemulsion; pea protein isolates; high-pressure homogenization; response surface methodology; ionic strength

1. Introduction

Consumers' preferences have drawn substantial scientific and industrial interest for the preparation of more natural and healthier foods [1–3]. The presence of both an aqueous phase and a lipid phase in foods is considered healthier, as the aqueous and lipid phases are responsible for the uptake of hydrophilic and lipophilic micronutrients in the gastrointestinal tract, respectively. As the majority of foods are naturally rich in aqueous phases, the dispersion of a certain amount of lipids in foods (e.g., soups, sauces, smoothies, purees, sausages, beverages, etc.) can significantly enhance the nutritional and sensory quality of foods by providing a suitable solvent system for lipophilic active components for enhanced stability, controlled release, and bioaccessibility [2–8]. The multi-phase system in which a liquid is dispersed in the continuous phase of (at least partly) immiscible liquid is referred to as an emulsion [9,10]. Systems with lipids/oils dispersed in the continuous aqueous phase are therefore referred to as oil-in-water (O/W) emulsions.

Emulsions with nanoscale droplet sizes are often referred to in the literature as mini emulsions, nanoemulsions, ultrafine emulsions, sub-micron emulsions, etc., and typically, those in the range of 20–100 nm radii are preferably referred to as nanoemulsions or ultrafine emulsions [3,11,12]. These droplets (r < 100 nm) are smaller than the wavelength of visible light (λ—390–750 nm), tend to be transparent or translucent to the naked eye, and possess stability against sedimentation or creaming [11–13]. Hence, these emulsions offer a promising application in the incorporation of lipophilic active components such

as micronutrients, flavors, nutraceuticals, or antimicrobials in aqueous-based foods or beverages that need to be optically transparent or at least translucent, e.g., fortified waters, soft drinks, sauces, and dips [12,13]. Nanoemulsions or ultrafine emulsions in the range of 20–50 nm radii could be referred to as ultra-nanoemulsions, which, because of their smaller size, can offer better stability, lightness, bioavailability, and control over the targeted delivery and release of active components [12–14].

With a dramatic increase in the interfacial area between immiscible liquids, emulsions are thermodynamically unstable and require an appropriate stabilizer to have a satisfactory (few weeks to months) shelf life without separating into independent phases via physicochemical mechanisms such as coalescence, creaming, and/or Ostwald ripening [2,15]. Conventional emulsions are stabilized by low-molecular surfactants, but in recent years, Pickering emulsions that are stabilized by solid particles are gaining popularity, with more reproducible formulations, reduced foaming problems, stimuli-responsiveness, and stability (against high oxidative, freeze–thaw, centrifugal, and thermal stress) as compared to those stabilized by surfactants [2,16,17]. Biomolecule-based particles, especially carbohydrates and proteins, have been regarded as promising emulsion stabilizers, whereas chemical and synthetic surfactants and/or inorganic particles are often criticized for causing irritation, damage to tissues, and environment-related issues [1,2,18,19].

Proteins are amphiphilic biopolymers, most of which can act as surfactants to stabilize emulsions via the hydrophilic–lipophilic dissolution balance. However, proteins can easily be transformed into Pickering particles by structural rearrangements in response to pH, ionic strength, and temperature and to stabilize emulsions via the hydrophilic–lipophilic adhesion–cohesion balance [15,20,21]. The net charge of a protein and its ability to rapidly reorient to the interface provide an opportunity for maximum interfacial coverage, which makes them potential candidates as good emulsion stabilizers [2,22]. Among the different proteins, pea (*Pisum sativum* L.) proteins stand out as common vegan, gluten-free, and low-allergenicity proteins [22], which makes them acceptable to a wide range of consumers, and they were therefore chosen as the nominated emulsion stabilizer in this study. Moreover, sunflower oil was used because of its light color and neutral flavor.

Although several methods are available for dispersing a lipid/oil phase in a continuous aqueous phase, not all of them can be used (easily) in a continuous process, especially with proteins due to their complex behavior at the interfaces in combination with the dynamic nature of the emulsification process [23]. For the production of nanoemulsions on an industrial scale, high-pressure homogenization (HPH) is still an attractive approach owing to its high throughput [24–26]. In general, the size of dispersed phase droplets in an emulsion produced by HPH can usually be decreased by increasing the homogenizer pressure or number of passes [26,27]. The major limitation of HPH for emulsification is the difficulty in controlling the droplet size distribution of dispersed phase droplets, which needs to be carefully optimized for commercial application [26,28].

Previous studies have revealed that pea protein isolates (PPIs) can satisfactorily stabilize emulsions alone [29,30] or in combination with other proteins [31,32] or polysaccharides [33–35] for the encapsulation and controlled release of lipophilic micronutrients. However, studies regarding the modeling and process optimization are limited. Response surface methodology (RSM) has been appreciated as a good statistical tool for establishing models and optimizing processing parameters with complex interactions [36] and has been used previously for the optimization of nanoemulsion composition and processing [37–39]. In this study, the optimization of a PPI-stabilized ultra-nanoemulsion (<100 nm) has been carried out in terms of PPI concentration (3–7%), sunflower oil content (4–10%), and homogenization pressure (20–40 MPa) by using response surface methodology (RSM). Afterwards, the optimum condition was predicted and validated. Finally, the effect of food matrix electrolytes, i.e., the pH and ionic strength, on the emulsion (prepared under optimized conditions) was evaluated.

2. Materials and Methods

2.1. Materials

Commercial food grade pea protein isolates (PPI) (80% protein) from MYVEGAN^{TM} UAE were used in this study. Sunflower oil (refractive index = 1.473) was purchased from a local grocery store. Deionized water (refractive index = 1.33) was used throughout the study.

2.2. Experimental Design and Evaluation

A central composite rotatable design (CCRD) with six center points was used to determine the combinations of three independent variables that were each present at five levels ($-\alpha$, -1, 0, 1, and $+\alpha$), as shown in Table 1. The center points and respective factorial points for PPI (5 ± 2%) and oil (7 ± 3%) were selected considering the solid-not-fat and fat percentage in milk of different origin as a reference, while the HPH pressure range (30 ± 10 MPa) was based on the results of previous studies [26,40]. Twenty experimental runs were generated, and three responses of droplet size distribution (i.e., Sauter mean diameter, median droplet diameter, and the span) were measured. The obtained responses were evaluated using response surface methodology. A quadratic polynomial model was fitted to each response using the following equation:

$$y = \beta_0 + \sum_{i=1}^{k} \beta_i X_i + \sum_{i=1}^{k} \beta_{ii} {X'}_i^2 + \sum_{i=1}^{k-1} \sum_{j=i+1}^{k} \beta_{ij} {X'}_i {X'}_j \tag{1}$$

where y is the response, β_0 is a constant, β_i is the linear coefficient, β_{ii} is the quadratic coefficient, β_{ij} is the interaction coefficient, k is the number of independent variables, β_i indicates the independent variables, and ${X'}_i$ and ${X'}_j$ indicate the difference between the independent variables and their respective center points. The optimization was carried out using the optimization settings presented in Table 2. Using the optimized factor conditions, the selected response was predicted and validated.

Table 1. Central composite rotatable design (CCRD) for the preparation of pea protein isolate (PPI)-stabilized sunflower oil in water nanoemulsions via high-pressure homogenization and the mean values for the responses viz. Sauter mean diameter ($D_{3,2}$), median droplet diameter (D_{50}), and span (δ).

Experimental Run	PPI %	Sunflower Oil %	Pressure (MPa)	$D_{3,2}$ (nm)	D_{50} (nm)	Span (δ)
1	7	4	40	90	200	3.95
2	3	4	40	97	220	3.5
3	5	7	30	108	279	3.34
4	5	7	30	106	275	4.09
5	5	7	30	100	245	3.91
6	7	10	40	114	268	3.07
7	5	7	30	104	258	3.76
8	7	4	20	107	288	4.14
9	5	1.95	30	85	181	4.07
10	5	7	30	102	259	3.99
11	3	10	20	103	298	4.69
12	5	7	13.18	135	488	4.03
13	3	10	40	131	328	4.72
14	5	7	30	104	262	3.71
15	5	12.05	30	110	298	3.85
16	3	4	20	125	368	3.71
17	1.64	7	30	144	521	11.62
18	5	7	46.82	102	227	3.31
19	8.36	7	30	101	239	3.66
20	7	10	20	109	329	11.77

Table 2. The optimization setting, optimized factor values, predicted value, and actual value for pea protein isolate (PPI)-stabilized nanoemulsions.

Optimization Setting			Optimized Factors Value			Predicted Value (nm)	Actual Value (nm)
Sauter Mean Diameter ($D_{3,2}$)	Values (nm)	Desirability	PPI (%)	Oil (%)	HPH Pressure (MPa)		
High	150	0.06				53.87 ± 34.23	80.53 ± 2.45
Middle	100	0.90	7.35	1.95	46.82		
Low	80	0.98					

2.3. Aqueous Phase, Coarse Emulsion, and Nanoemulsion Preparation

PPI (1.64–8.36%) was dispersed in deionized water, magnetically stirred (650 rpm) at room temperature for 60 min, and left undisturbed at 4 °C overnight. PPI solution was centrifuged (10,000× *g*; 30 min at 4 °C) to obtain the supernatant; the supernatant was centrifuged again under the previous conditions to obtain the final supernatant, which was then used as the aqueous phase for coarse emulsion preparation.

Sunflower oil (1.95–12.05%), which was added to the aqueous phase and coarse emulsion, was prepared via homogenization at 10,000 rpm for 2 min using ULTRA-TURRAX (T25 D, IKA®-Werke GmbH & Co. KG, Staufen, Germany) with an 18 G probe. The nanoemulsions were produced by passing the coarse emulsions through a high-pressure homogenizer (FT90, Armfield Ltd., UK) 3 times with a pressure of 13.18–46.82 MPa. In addition to the samples required for CCRD, the nanoemulsions were also prepared under optimum process conditions with different ionic strengths (0–400 mM NaCl in the aqueous phase) and with different pH values (3, 5, and 7 pH of the aqueous phase, adjusted using 1 N solutions of HCl and NaOH). The aqueous phases with different ionic strengths and pH values were also kept overnight at 4 °C prior to emulsification.

2.4. Emulsion Characterization

All nanoemulsions were characterized for droplet size distribution using a laser diffraction particle size analyzer (Malvern Mastersizer 3000, Malvern Panalytical Ltd., Malvern, UK). The refractive indices of 1.46 and 1.33 were entered into the machine's SOP for sunflower oil and continuous phase, respectively. An emulsion sample was slowly added (using a 3 mL bubble pipette) into the wet sample dispersion unit (Hydro EV) containing deionized water until a 10% obscuration level was reached, and then, the measurement cycle was run to record the droplet size distribution. From each measurement (an average of three readings), the Sauter mean diameter ($D_{3,2}$), median diameter (D_{50}), and span value (δ) were taken for further analysis. The Sauter mean diameter (also known as surface-volume mean diameter) can be defined as

$$D_{3,2} = \frac{\sum_{i=1}^{n} n_i D_i^3}{\sum_{i=1}^{n} n_i D_i^2} \tag{2}$$

where n_i and D_i are the number and diameters of emulsion droplets in a particular size fraction [41], whereas the median diameter corresponds to a size when the cumulative droplet size distribution reaches 50% (Figure 1). Furthermore, the span value was used to describe the width of droplet size distribution (i.e., the polydispersity of the emulsion), which can be defined as

$$\delta = \frac{D_{90} - D_{10}}{D_{50}} \tag{3}$$

where D_{10}, D_{50}, and D_{90} are the droplet sizes corresponding to a cumulative droplet size distribution of 10%, 50%, and 90%, respectively (Figure 1).
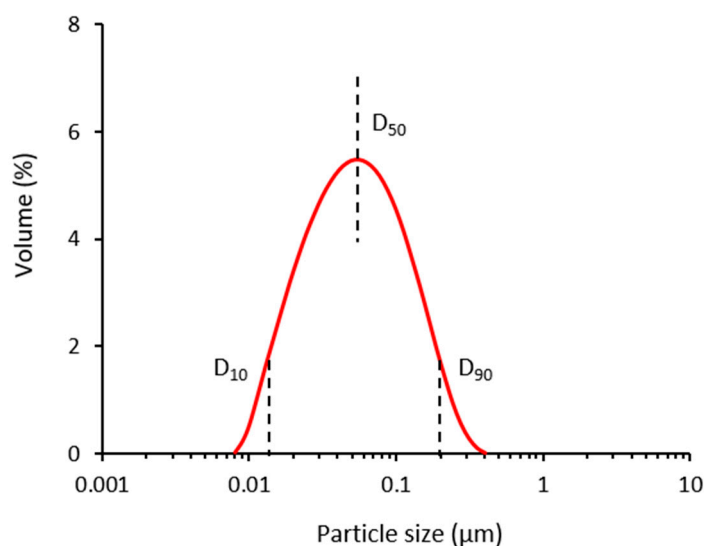
Figure 1. A typical size distribution curves representing D_{10}, D_{50}, and D_{90}.

The emulsions were then stored at refrigeration temperature (~4 °C) in capped glass bottles (500 mL). In order to determine the stability of emulsions, the samples were analyzed again for droplet size distribution after a week using the same protocol as described above.

2.5. Statistical Analysis

JMP PRO 15 software (SAS Institute Inc., Cary, NC, USA) was used to develop the experimental design and to evaluate independent variables via response surface methodology and optimization. The Tukey-HSD test was used for the mean comparison wherever applicable.

3. Results and Discussion

3.1. Response Surface Evaluation

Response surface evaluation for each of the emulsion characteristics viz. the Sauter mean diameter ($D_{3,2}$), median diameter (D_{50}), and the span value (δ) was carried out, and the response surface coefficients, coefficient of determination (R^2), and significance of regression (p-value) were determined (Table 3). The evaluation revealed that the main effects of PPI (%) and oil (%), the quadratic effect of PPI (%), and interaction between the oil (%) and HPH pressure (MPa) had significant effects ($p < 0.05$) on $D_{3,2}$, whilst only the main effects of PPI (%) and HPH pressure (MPa) had significant effects ($p < 0.05$) on D_{50}. No significant effect ($p > 0.05$) of the evaluated factors was observed for the span; however, the quadratic effect of PPI (%) was significant at a 10% level of significance. The interaction plots for each of the emulsion characteristics are presented in Figure 2.

Table 3. Response surface coefficients, coefficient of determination (R^2), and significance of models (p-value) for the Sauter mean diameter ($D_{3,2}$), median droplet diameter (D_{50}), and span (δ) of pea protein isolate (PPI)-stabilized nanoemulsions via high-pressure homogenization (HPH).

Factors	Constant	A	B	C	D	E	F	G	H	I	R^2 (%)	Model p-Value
$D_{3,2}$	125.11 ***	−3.97 ***	1.95 **	−0.49 *	1.43 **	−0.35	0.04 *	0.29	−0.08	0.33 ***	83	<0.005
D_{50}	471.15 ***	−22.09 **	8.39	−5.17 **	8.13 *	−1.91	0.25	1.48	−0.19	0.85	77	<0.05
Span	5.895	−0.26	0.21	−0.08	0.33	0.00	−0.00	0.09	−0.05	−0.03	55	NS

A, B, C, D, E, F, G, H, and I are the coefficients for PPI, oil, HPH pressure, $(\text{PPI}—5)^2$, $(\text{oil}—7)^2$, $(\text{HPH pressure}—30)^2$, $(\text{PPI}—5)$ $(\text{oil}—7)$, $(\text{PPI}—5)$ $(\text{HPH pressure}—30)$, and $(\text{oil}—7)$ $(\text{HPH pressure}—30)$, respectively. * $p < 0.1$; ** $p < 0.05$, *** $p < 0.005$.
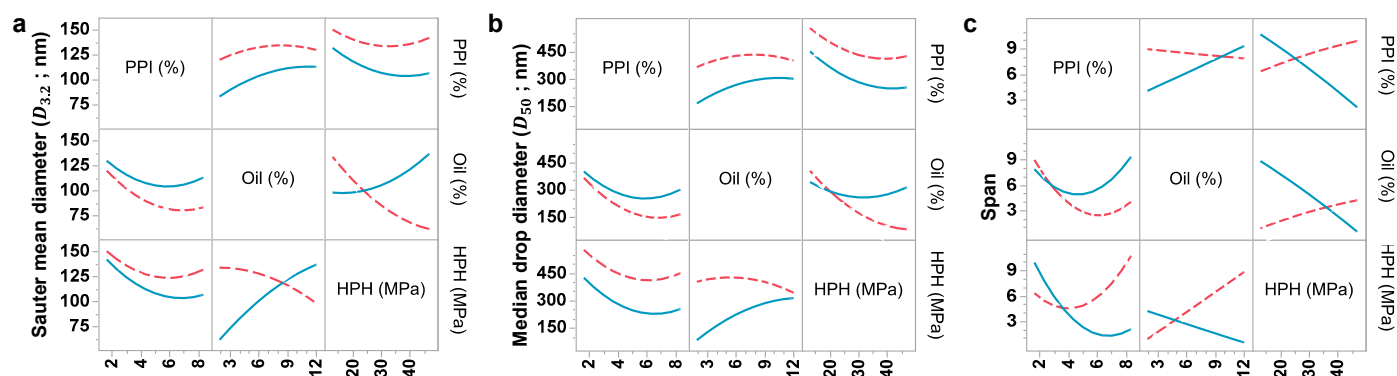
Figure 2. Interaction profiler chart for the response surface evaluation of the emulsion characteristics: (**a**) Sauter mean diameter, (**b**) median droplet diameter, and (**c**) span of pea protein isolate (PPI)-stabilized nanoemulsions. Continuous and discontinuous lines indicate the high-level and low-level conditions, respectively, for the parameter shown on secondary (right) *y*-axis.

3.1.1. Effect of PPI Concentration

In general, droplets' sizes reduce with higher PPI concentrations, and a similar behavior was observed in the current study. In fact, a limited particle concentration resulted in the insufficient interfacial coverage of droplets, which led to bridge flocculation and ultimately to coalescence [31,42–44]. This was also evident from a higher span value (due to a wider droplet size distribution, or in some cases due to a bi-modal distribution) for those emulsion samples containing lower PPI concentrations. At extreme poor coverage of the interface, emulsification failure occurred [42], although this was not observed in any of the emulsification runs in the present study.

With the increase in PPI concentration, a gradual decrease in the droplets' size was observed. The decrease in droplet size with the increase in particle concentration has been reported previously [31,45–47] and is valid until the maximum critical particle concentration is reached, beyond which, the increase in particle concentration contributes to the viscosity and density and subsequent emulsion stability [2,42,43]. For low oil content and high HPH pressure, the maximum critical particle concentration was ~6%, i.e., a further increase in PPI concentration did not show a further decrease in droplet size. However, for high oil content and low HPH pressure, the increase in PPI (beyond 6%) resulted in a slight increase in the droplet size with a very high span. This could be associated with more than one factor, most likely due to an increased coalescence probability at higher oil content immediately after droplet disruption [48] and/or due to an incomplete homogenization as a result of (i) an overall increase in emulsion viscosity and (ii) a decrease in the flow velocity of the emulsion in the dispersing zone [49,50]. This was also indicated by a higher span value of the respective emulsion samples. The large-sized droplets at high PPI concentrations could also be partly associated with the depletion flocculation [31]. Hence, the desired droplets of <100 nm could only be achieved at a high PPI concentration (~6%), with less oil content using high HPH pressure.

3.1.2. Effect of Oil Content

The increase in dispersed phase in general results in an increase in the droplets' size [51,52], which was also evident in our results. Such an increase in droplets' size can occur due to an increase in the interfacial area, limiting the stabilizer with an increase in the oil content, as also explained in the above section. In addition, the increase in oil content is followed by a decrease in the aqueous continuous phase, which results in the decrease in the total stabilizer concentration of the system, especially when stabilizers are dispersed in the aqueous phase. The reduction in the effective stabilizer concentration to oil ratio results in large droplets with wide distribution and low stability [53–55]. In this study, as the PPI was present in the aqueous phase, the increase in oil content led to the decrease in the effective PPI concentration in the total emulsion system, limiting the particles, which

could explain the increase in droplets' size with the increase in oil content. However, in some cases, the increase in dispersed phase can reduce the droplets' size, for instance, when the stabilizers were present in the dispersed phase [56] or when the stabilizer is in sufficiently high concentration in the continuous phase [51,57]. However, at low HPH pressure, the increase in oil content resulted in a slight reduction in the droplets' size. This could possibly be associated with droplet disruption due to an increased probability of liquid–liquid interactions (indirect breaking) at low flow velocities [58]. However, this can also be regarded as an incomplete homogenization which is also evident from a high D_{50} and a very high span value as compared to those at high HPH pressure.

3.1.3. Effect of HPH Pressure

In general, the increase in HPH pressure increases the degree of emulsification and results in smaller-sized droplets [9,59]. In this study, the increase in HPH pressure also resulted in the decrease in the droplets' size, but only when the PPI was present in a sufficiently high concentration or when the oil content was low. High HPH pressure corresponds to a high energy density in the dispersing zone, which results in a smaller droplet size. However, the newly created interfacial area should be immediately stabilized; otherwise, the disruption results will be superimposed by coalescence [50]. This explains the effectiveness of high HPH pressure to produce nanoemulsions at high PPI concentrations or low oil fractions, with the former being more important. At a low PPI concentration, the increase in HPH pressure had a negligible effect on $D_{3,2}$, while D_{50} followed the general trend. This could be associated with the inadequate stabilization of droplets, resulting in a bimodal distribution, as evidenced by a high span value. Furthermore, provided the sufficient availability of stabilizer, a higher oil fraction (up to 7%) can also be well homogenized into nanoemulsion (while considering droplet size and span value together) even at a moderate HPH pressure (~35 MPa).

The reduction in droplets' size with increasing HPH pressure could partly be associated with protein modification (although it was not the aim of present investigation). The state of a protein significantly influences its emulsifying properties [60]. Several studies have revealed that the increase in HPH pressure can physically modify proteins to improve their emulsifying and stabilizing properties and thus can stabilize smaller-sized droplets at the same particle concentration [26,61–63].

3.2. Prediction and Validation

The coefficient of determination for the median droplet diameter (D_{50}) and the span value (δ) were below 80% and were more likely to deviate away from the predicted values. Increasing the number of runs or further customization of the model could potentially improve the coefficient of determination. However, a good coefficient of determination and a highly significant response surface model was obtained for $D_{3,2}$. Therefore, optimization was carried out to minimize $D_{3,2}$ below 100 nm. The optimization setting and optimized factor values for the nanoemulsions are presented in Table 2. The actual value of 80.53 ± 2.45 nm was within the upper range of the prediction value of 53.87 ± 34.23. Hence, the response surface model can efficiently be used to optimize the PPI-stabilized nanoemulsions and to predict $D_{3,2}$ within the experimental range of the study.

3.3. Emulsion Stability

Out of 20 emulsification runs shown in Table 1, 10 emulsion samples (having $D_{3,2} \leq 100$ nm) were selected for a short-term stability study to further explain the suitability of emulsification conditions. The selected samples were stored at 4 °C, and then, their droplet size distributions were again analyzed after 7 days. The change in droplet size between day 0 and day 7 is graphically shown in Figure 3a, where each data point represents the average $D_{3,2}$ of the selected emulsification runs. It can be visualized that for the majority of emulsification conditions, a non-significant change ($p > 0.05$) in average $D_{3,2}$ was observed between day 0 and day 7. However, the data points for day 7 seem to be

more scattered than those for day 0. This is further explained by plotting $D_{3,2}$ (for Day 7) as a function of the PPI-to-Oil ratio (P/O) and HPH pressure used during the emulsification of respective samples (Figure 3b). A clear trend in the reduction in $D_{3,2}$ can be seen with the increase in HPH pressure; and furthermore, a high P/O resulted in the better stability of the nanoemulsions, which is again in accordance with the discussion presented in Section 3.1. In addition to HPH pressure and P/O ratio, another aspect of nanoemulsions' stability is their extremely small droplet size, which is evident from some data points ($D_{3,2} \leq 100$ nm), but the samples were still stable at a relatively lower P/O ratio. In fact, the nanosized emulsion droplets usually have better stability against coalescence [2,64]; specifically, they have a low collision probability at a low dispersed phase fraction [65,66]. Therefore, the droplet sizes for these samples did not grow significantly even after 7 days.
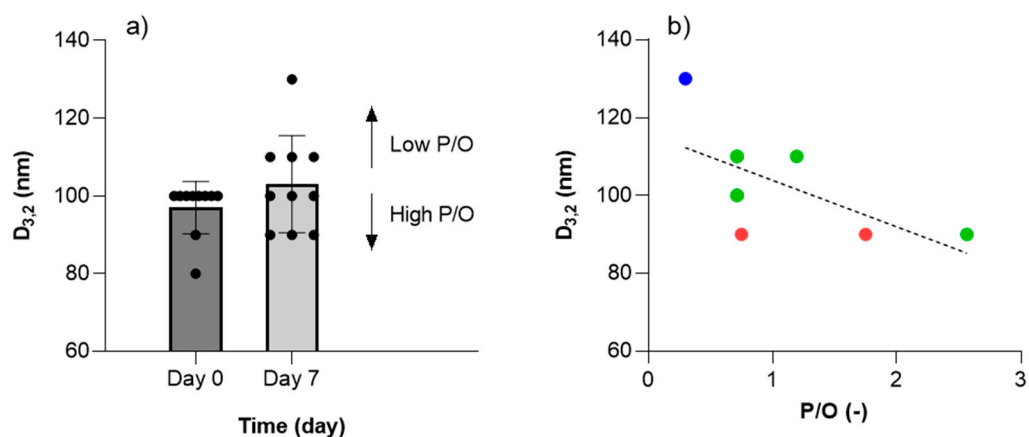

Figure 3. (**a**) Sauter mean diameter ($D_{3,2}$) of nanoemulsions (<100 nm) as a function of time, and (**b**) ($D_{3,2}$) at day 7 as a function of PPI-to-Oil ratio (P/O) and HPH pressure: 200 MPa (blue), 300 MPa (green), and 400 MPa (red).

3.4. Effect of Salt on Optimized Conditions

For the optimized set of factor values, the size distribution characteristics of emulsions at different concentrations of salt in the range of most food applications (0–400 mM) were evaluated and are presented in Figure 4a–c. The droplets' sizes for all emulsions were <100 nm. When a small amount (25 mM) of salt was present in the aqueous phase, the size of emulsion droplets was reduced, but a further increase in the salt concentration (200–400 mM) resulted in the formation of droplets with slightly bigger diameters. Additionally, the span value decreased initially with the increase in NaCl from 0 to 50 mM, beyond which, a significant increase in span was observed. Very low salt concentrations are in general favorable to emulsions, while a further increase in the salt concentration can reduce the electrostatic repulsion between the particles, resulting in some particle aggregation, which can increase the effective particle size at the interface and thus the size of emulsion droplets [2,67]. Despite the reduction in electrostatic repulsions, no phase separation or flocs were seen, indicating that the main force involved in the stabilization of emulsions using PPI was steric repulsion rather than electrostatic repulsion [46,68]. The slight increase in droplets' diameter at 200–400 mM NaCl could also be due to the coalescence of smaller droplets under the effect of strong electrostatic screening [46,69]. It is, however, important to note that the optimum salt concentrations for an emulsion preparation and their effect could depend on the type of salt in itself and the salt susceptibility of the proteins at the given pH [2,70,71].
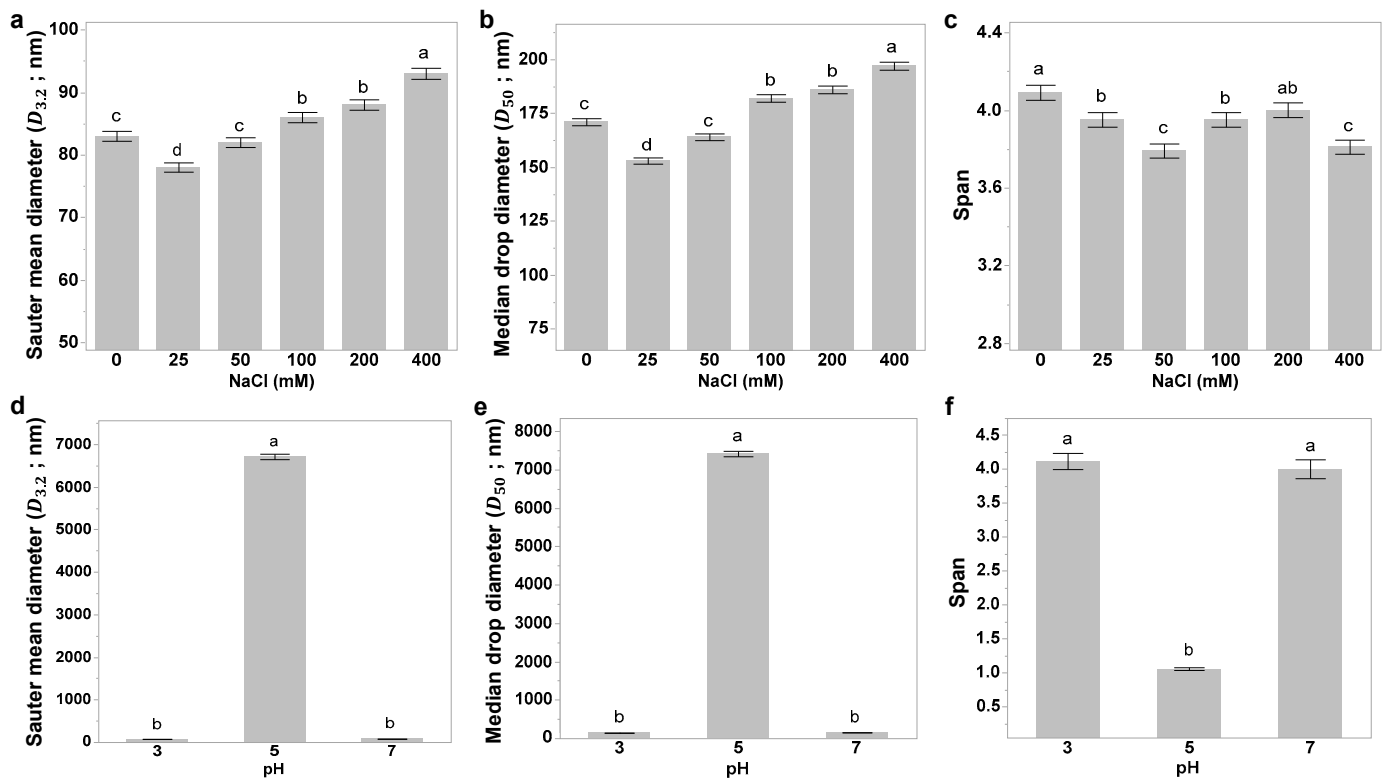
Figure 4. Emulsion characteristics (Sauter mean diameter, median droplet diameter, and span) of pea protein isolate-stabilized nanoemulsions at different NaCl solutions (**a**–**c**) and at different pH conditions (**d**–**f**). Different alphabets above the error bars indicate significant difference among sample means at $p < 0.05$.

3.5. Effect of pH on Optimized Emulsion

For the optimized set of factor values, the emulsion droplet size characteristics of emulsions ($D_{3,2}$, D_{50}, and δ) at different pH values are presented in Figure 4d–f. The emulsions prepared at pH 3 and 7 resulted in very fine droplets, whilst near the isolectric point (pI), i.e., pH 5, relatively larger droplets were formed. Near the pI, the protein particles lose their charge and electrostatic repulsion, and thus tend to form aggregates [2]. The aggregated particles will eventually form larger-sized droplets, as the size of droplets is significantly influenced by the size of particles. The smallest size of droplet that a particle can stabilize is its own size [2], although some reports are available in which the droplets smaller than the initial particle size were stabilized; however, it was suggested that the sizes of particles were reduced during the emulsification, and the droplets' sizes were larger than the sizes of effective particles at the interface [72,73].

The emulsions prepared at pH 3 and 7 were far smaller than those at pH 5. At pH 7, PPI have a high negative charge, low hydrophobicity, and high solubility, which allow them to associate better with the oil–water interface to lower interfacial tension [74]. In contrast, at pH 3, PPI possess high positive charge, high hydrophobicity, and high solubility, which leads to the formation of stronger interfacial viscoelastic films [30,74]. While some studies have revealed that the emulsions formed at pH 3 formed smaller droplets [30,75,76] and much better interfacial rheology [74], the emulsions prepared under both of these conditions (pH 3 and 7) were statistically similar. The better results of PPI at pH 3 were suggested to be due to the ability of PPI to possess a smaller hydrodynamic diameter (134–165 nm) [30]. In this study, emulsions with droplets' size <100 nm were prepared, which implies that the effective size of PPI particles is much smaller than the suggested size, possibly due to the impact of high HPH pressure on PPI size and emulsion stabilization properties [26,61–63].

4. Conclusions

Response surface methodology can be effectively used to optimize PPI-stabilized O/W ultra-nanoemulsions of Sauter mean diameter ($D_{3,2}$) < 100 nm. The droplets' size was mainly influenced by the PPI concentration and the interaction of oil content and HPH pressure. The increase in PPI concentration and HPH pressure reduced the emulsions' droplets' size, while the increase in oil fraction had a slight tendency to increase the emulsions' droplets' size. The span values of the emulsion droplets were high for a very low PPI concentration and for the combination of high oil fraction and low HPH pressure. The prepared emulsions were stable, as no significant difference in the emulsions size distribution was observed when these emulsions were evaluated on day 7. The desired emulsions (<100 nm) were optimized at 6.45% PPI, with 1.95% oil and at 46.82 HPH pressure. The emulsions prepared under such conditions were capable of maintaining the droplets' size <100 nm even when the ionic conditions were altered with up to 400 mM NaCl and the pH was adjusted to 3 or 7. However, micro-emulsions were formed at pH 5. The encapsulation and bioaccessibility studies of lipophilic micronutrients could further elaborate upon the potentials of PPI for use in the industrial preparation of such nanoemulsions.

Author Contributions: The manuscript was written through the contributions of all authors. A.N. (Anuj Niroula): Methodology, Writing—Original Draft. R.A.: Investigation. B.S.: Investigation, Methodology, Supervision. A.N. (Akmal Nazir): Conceptualization, Supervision, Writing—Review and Editing. All authors have read and agreed to the published version of the manuscript.

Institutional Review Board Statement: Not applicable.

Informed Consent Statement: Not applicable.

Data Availability Statement: The data presented in this study are available on request from the corresponding author.

Conflicts of Interest: The authors declare no conflict of interest.

References

1. Santiago, J.S.J.; Salvia-Trujillo, L.; Palomo, A.; Niroula, A.; Xu, F.; Van Loey, A.; Hendrickx, M.E. Process-induced water-soluble biopolymers from broccoli and tomato purées: Their molecular structure in relation to their emulsion stabilizing capacity. *Food Hydrocoll.* **2018**, *81*, 312–327. [CrossRef]
2. Niroula, A.; Gamot, T.D.; Ooi, C.W.; Dhital, S. Biomolecule-based pickering food emulsions: Intrinsic components of food matrix, recent trends and prospects. *Food Hydrocoll.* **2020**, *112*, 106303. [CrossRef]
3. Chung, C.; McClements, D.J. Structure–function relationships in food emulsions: Improving food quality and sensory perception. *Food Struct.* **2013**, *1*, 106–126. [CrossRef]
4. Ma, Z.; Khalid, N.; Shu, G.; Zhao, Y.; Kobayashi, I.; Neves, M.A.; Tuwo, A.; Nakajima, M. Fucoxanthin-Loaded Oil-in-Water Emulsion-Based Delivery Systems: Effects of Natural Emulsifiers on the Formulation, Stability, and Bioaccessibility. *ACS Omega* **2019**, *4*, 10502–10509. [CrossRef] [PubMed]
5. Iqbal, R.; Mehmood, Z.; Baig, A.; Khalid, N. Formulation and characterization of food grade O/W nanoemulsions encapsulating quercetin and curcumin: Insights on enhancing solubility characteristics. *Food Bioprod. Process.* **2020**, *123*, 304–311. [CrossRef]
6. Kaade, W.; Méndez-Sánchez, C.; Güell, C.; De Lamo-Castellví, S.; Mestres, M.; Ferrando, M. Complexed Biopolymer of Whey Protein and Carboxymethyl Cellulose to Enhance the Chemical Stability of Lemon Oil-in-Water Emulsions. *ACS Food Sci. Technol.* **2022**, *2*, 41–48. [CrossRef]
7. Lam, R.S.H.; Nickerson, M.T. Food proteins: A review on their emulsifying properties using a structure–function approach. *Food Chem.* **2013**, *141*, 975–984. [CrossRef]
8. Drapala, K.P.; Mulvihill, D.M.; O'Mahony, J.A. A review of the analytical approaches used for studying the structure, interactions and stability of emulsions in nutritional beverage systems. *Food Struct.* **2018**, *16*, 27–42. [CrossRef]
9. Tadros, T.F. *Emulsion Formation, Stability, and Rheology*; John Wiley & Sons, Ltd.: Hoboken, NJ, USA, 2013; pp. 1–75. [CrossRef]
10. McClements, D.J. *Biopolymers in Food Emulsions*; Kasapis, S., Norton, I.T., Ubbink, J.B., Eds.; Elsevier Inc.: Amsterdam, The Netherlands, 2009; pp. 129–166. [CrossRef]
11. Solans, C.; Izquierdo, P.; Nolla, J.; Azemar, N.; Garcia-Celma, M. Nano-emulsions. *Curr. Opin. Colloid Interface Sci.* **2005**, *10*, 102–110. [CrossRef]

12. Yang, Y.; Marshall-Breton, C.; Leser, M.E.; Sher, A.A.; McClements, D.J. Fabrication of ultrafine edible emulsions: Comparison of high-energy and low-energy homogenization methods. *Food Hydrocoll.* **2012**, *29*, 398–406. [CrossRef]
13. Velikov, K.P.; Pelan, E. Colloidal delivery systems for micronutrients and nutraceuticals. *Soft Matter* **2008**, *4*, 1964–1968. [CrossRef]
14. Araiza-Calahorra, A.; Akhtar, M.; Sarkar, A. Recent advances in emulsion-based delivery approaches for curcumin: From encapsulation to bioaccessibility. *Trends Food Sci. Technol.* **2018**, *71*, 155–169. [CrossRef]
15. McClements, D.J. Lipid-Based Emulsions and Emulsifier. In *Food Lipids*, 4th ed.; Akoh, C.C., Ed.; CRC Press: Boca Raton, FL, USA, 2008; pp. 64–96.
16. Tenorio-Garcia, E.; Araiza-Calahorra, A.; Simone, E.; Sarkar, A. Recent advances in design and stability of double emulsions: Trends in Pickering stabilization. *Food Hydrocoll.* **2022**, *128*, 107601. [CrossRef]
17. Xia, T.; Xue, C.; Wei, Z. Physicochemical characteristics, applications and research trends of edible Pickering emulsions. *Trends Food Sci. Technol.* **2020**, *107*, 1–15. [CrossRef]
18. Berton-Carabin, C.C.; Schroën, K. Pickering Emulsions for Food Applications: Background, Trends, and Challenges. *Annu. Rev. Food Sci. Technol.* **2015**, *6*, 263–297. [CrossRef]
19. Zhou, B.; Gao, S.; Li, X.; Liang, H.; Li, S. Antioxidant Pickering emulsions stabilised by zein/tannic acid colloidal particles with low concentration. *Int. J. Food Sci. Technol.* **2019**, *55*, 1924–1934. [CrossRef]
20. Ferdous, S.; Ioannidis, M.A.; Henneke, D.E. Effects of temperature, pH, and ionic strength on the adsorption of nanoparticles at liquid–liquid interfaces. *J. Nanoparticle Res.* **2012**, *14*, 850. [CrossRef]
21. Murray, B.S. Pickering emulsions for food and drinks. *Curr. Opin. Food Sci.* **2019**, *27*, 57–63. [CrossRef]
22. Lam, A.C.Y.; Can Karaca, A.; Tyler, R.T.; Nickerson, M.T. Pea protein isolates: Structure, extraction, and functionality. *Food Rev. Int.* **2018**, *34*, 126–147. [CrossRef]
23. Güell, C.; Ferrando, M.; Trentin, A.; Schroën, K. Apparent Interfacial Tension Effects in Protein Stabilized Emulsions Prepared with Microstructured Systems. *Membranes* **2017**, *7*, 19. [CrossRef]
24. Köhler, K.; Santana, A.S.; Braisch, B.; Preis, R.; Schuchmann, H. High pressure emulsification with nano-particles as stabilizing agents. *Chem. Eng. Sci.* **2010**, *65*, 2957–2964. [CrossRef]
25. Donsì, F.; Senatore, B.; Huang, Q.; Ferrari, G. Development of Novel Pea Protein-Based Nanoemulsions for Delivery of Nutraceuticals. *J. Agric. Food Chem.* **2010**, *58*, 10653–10660. [CrossRef] [PubMed]
26. Morales, E.; Burgos-Díaz, C.; Zúñiga, R.; Jorkowski, J.; Quilaqueo, M.; Rubilar, M. Effect of Interfacial Ionic Layers on the Food-Grade O/W Emulsion Physical Stability and Astaxanthin Retention during Spray-Drying. *Foods* **2021**, *10*, 312. [CrossRef] [PubMed]
27. Soo, Y.N.; Tan, C.P.; Tan, P.Y.; Khalid, N.; Tan, T.B. Fabrication of oil-in-water emulsions as shelf-stable liquid non-dairy creamers: Effects of homogenization pressure, oil type, and emulsifier concentration. *J. Sci. Food Agric.* **2020**, *101*, 2455–2462. [CrossRef] [PubMed]
28. Van Der Graaf, S.; Schroen, K.; Boom, R. Preparation of double emulsions by membrane emulsification—A review. *J. Membr. Sci.* **2005**, *251*, 7–15. [CrossRef]
29. Shao, Y.; Tang, C.-H. Gel-like pea protein Pickering emulsions at pH3.0 as a potential intestine-targeted and sustained-release delivery system for β-carotene. *Food Res. Int.* **2016**, *79*, 64–72. [CrossRef]
30. Liang, H.-N.; Tang, C.-H. Pea protein exhibits a novel Pickering stabilization for oil-in-water emulsions at pH 3.0. *LWT* **2014**, *58*, 463–469. [CrossRef]
31. Hinderink, E.B.; Münch, K.; Sagis, L.; Schroën, K.; Berton-Carabin, C. Synergistic stabilisation of emulsions by blends of dairy and soluble pea proteins: Contribution of the interfacial composition. *Food Hydrocoll.* **2019**, *97*, 105206. [CrossRef]
32. Hinderink, E.B.A.; Berton-Carabin, C.C.; Schroën, K.; Riaublanc, A.; Houinsou-Houssou, B.; Boire, A.; Genot, C. Conformational Changes of Whey and Pea Proteins upon Emulsification Approached by Front-Surface Fluorescence. *J. Agric. Food Chem.* **2021**, *69*, 6601–6612. [CrossRef]
33. Feng, T.; Wang, X.; Wang, X.; Zhang, X.; Gu, Y.; Xia, S.; Huang, Q. High internal phase pickering emulsions stabilized by pea protein isolate-high methoxyl pectin-EGCG complex: Interfacial properties and microstructure. *Food Chem.* **2021**, *350*, 129251. [CrossRef]
34. Wang, T.; Zhang, W.; Li, L.; Zhang, H.; Feng, W.; Wang, R. Protein networks and starch nanocrystals jointly stabilizing liquid foams via pickering-type coverages and steric hindrance. *Food Chem.* **2021**, *370*, 131014. [CrossRef] [PubMed]
35. Yi, J.; Huang, H.; Liu, Y.; Lu, Y.; Fan, Y.; Zhang, Y. Fabrication of curcumin-loaded pea protein-pectin ternary complex for the stabilization and delivery of β-carotene emulsions. *Food Chem.* **2019**, *313*, 126118. [CrossRef] [PubMed]
36. Yolmeh, M.; Jafari, S.M. Applications of Response Surface Methodology in the Food Industry Processes. *Food Bioprocess Technol.* **2017**, *10*, 413–433. [CrossRef]
37. Katsouli, M.; Polychniatou, V.; Tzia, C. Optimization of water in olive oil nano-emulsions composition with bioactive compounds by response surface methodology. *LWT* **2018**, *89*, 740–748. [CrossRef]
38. Raviadaran, R.; Chandran, D.; Shin, L.H.; Manickam, S. Optimization of palm oil in water nano-emulsion with curcumin using microfluidizer and response surface methodology. *LWT* **2018**, *96*, 58–65. [CrossRef]
39. Pongsumpun, P.; Iwamoto, S.; Siripatrawan, U. Response surface methodology for optimization of cinnamon essential oil nanoemulsion with improved stability and antifungal activity. *Ultrason. Sonochem.* **2019**, *60*, 104604. [CrossRef]

40. Li, Y.; Xiang, D. Stability of oil-in-water emulsions performed by ultrasound power or high-pressure homogenization. *PLoS ONE* **2019**, *14*, e0213189. [CrossRef]

41. Kowalczuk, P.B.; Drzymala, J. Physical meaning of the Sauter mean diameter of spherical particulate matter. *Part. Sci. Technol.* **2015**, *34*, 645–647. [CrossRef]

42. Frelichowska, J.; Bolzinger, M.-A.; Chevalier, Y. Effects of solid particle content on properties of o/w Pickering emulsions. *J. Colloid Interface Sci.* **2010**, *351*, 348–356. [CrossRef]

43. Sun, Z.; Yan, X.; Xiao, Y.; Hu, L.; Eggersdorfer, M.; Chen, D.; Yang, Z.; Weitz, D.A. Pickering emulsions stabilized by colloidal surfactants: Role of solid particles. *Particuology* **2022**, *64*, 153–163. [CrossRef]

44. Tcholakova, S.; Denkov, N.D.; Lips, A. Comparison of solid particles, globular proteins and surfactants as emulsifiers. *Phys. Chem. Chem. Phys.* **2008**, *10*, 1608–1627. [CrossRef]

45. Aluko, R.E.; Mofolasayo, O.A.; Watts, B.M. Emulsifying and foaming properties of commercial yellow pea (Pisum sativum L.) seed flours. *J. Agric. Food Chem.* **2009**, *57*, 9793–9800. [CrossRef] [PubMed]

46. Li, X.-L.; Liu, W.-J.; Xu, B.-C.; Zhang, B. Simple method for fabrication of high internal phase emulsions solely using novel pea protein isolate nanoparticles: Stability of ionic strength and temperature. *Food Chem.* **2021**, *370*, 130899. [CrossRef] [PubMed]

47. Tcholakova, S.; Denkov, N.D.; Ivanov, I.B.; Campbell, B. Coalescence stability of emulsions containing globular milk proteins. *Adv. Colloid Interface Sci.* **2006**, *123–126*, 259–293. [CrossRef] [PubMed]

48. Nazir, A.; Schroën, K.; Boom, R. High-throughput premix membrane emulsification using nickel sieves having straight-through pores. *J. Membr. Sci.* **2011**, *383*, 116–123. [CrossRef]

49. Liu, C.; Fan, L.; Yang, Y.; Jiang, Q.; Xu, Y.; Xia, W. Characterization of surimi particles stabilized novel pickering emulsions: Effect of particles concentration, pH and NaCl levels. *Food Hydrocoll.* **2021**, *117*, 106731. [CrossRef]

50. Brösel, S.; Schubert, H. Investigations on the role of surfactants in mechanical emulsification using a high-pressure homogenizer with an orifice valve. *Chem. Eng. Process. Process Intensif.* **1999**, *38*, 533–540. [CrossRef]

51. Hadnađev, T.D.; Dokić, P.; Krstonošić, V.; Hadnađev, M. Influence of oil phase concentration on droplet size distribution and stability of oil-in-water emulsions. *Eur. J. Lipid Sci. Technol.* **2012**, *115*, 313–321. [CrossRef]

52. Buyukkestelli, H.I.; El, S.N. Preparation and characterization of double emulsions for saltiness enhancement by inhomogeneous spatial distribution of sodium chloride. *LWT* **2018**, *101*, 229–235. [CrossRef]

53. Wang, J.; Shi, A.; Agyei, D.; Wang, Q. Formulation of water-in-oil-in-water (W/O/W) emulsions containing trans-resveratrol. *RSC Adv.* **2017**, *7*, 35917–35927. [CrossRef]

54. Xiao, J.; Lu, X.; Huang, Q. Double emulsion derived from kafirin nanoparticles stabilized Pickering emulsion: Fabrication, microstructure, stability and in vitro digestion profile. *Food Hydrocoll.* **2017**, *62*, 230–238. [CrossRef]

55. Li, M.-F.; He, Z.-Y.; Li, G.-Y.; Zeng, Q.-Z.; Su, D.-X.; Zhang, J.-L.; Wang, Q.; Yuan, Y.; He, S. The formation and characterization of antioxidant pickering emulsions: Effect of the interactions between gliadin and chitosan. *Food Hydrocoll.* **2018**, *90*, 482–489. [CrossRef]

56. Qin, X.-S.; Luo, Z.-G.; Li, X.-L. An enhanced pH-sensitive carrier based on alginate-Ca-EDTA in a set-type W1/O/W2 double emulsion model stabilized with WPI-EGCG covalent conjugates for probiotics colon-targeted release. *Food Hydrocoll.* **2020**, *113*, 106460. [CrossRef]

57. Buyukkestelli, H.I.; El, S.N. Development and characterization of double emulsion to encapsulate iron. *J. Food Eng.* **2019**, *263*, 446–453. [CrossRef]

58. Nazir, A.; Vladisavljević, G.T. Droplet breakup mechanisms in premix membrane emulsification and related microfluidic channels. *Adv. Colloid Interface Sci.* **2021**, *290*, 102393. [CrossRef] [PubMed]

59. Schultz, S.; Wagner, G.; Urban, K.; Ulrich, J. High-Pressure Homogenization as a Process for Emulsion Formation. *Chem. Eng. Technol.* **2004**, *27*, 361–368. [CrossRef]

60. Geerts, M.E.; Nikiforidis, C.V.; van der Goot, A.J.; van der Padt, A. Protein nativity explains emulsifying properties of aqueous extracted protein components from yellow pea. *Food Struct.* **2017**, *14*, 104–111. [CrossRef]

61. Primozic, M.; Duchek, A.; Nickerson, M.; Ghosh, S. Formation, stability and in vitro digestibility of nanoemulsions stabilized by high-pressure homogenized lentil proteins isolate. *Food Hydrocoll.* **2018**, *77*, 126–141. [CrossRef]

62. Ma, W.; Wang, J.; Wu, D.; Xu, X.; Wu, C.; Du, M. Physicochemical properties and oil/water interfacial adsorption behavior of cod proteins as affected by high-pressure homogenization. *Food Hydrocoll.* **2019**, *100*, 105429. [CrossRef]

63. Luo, L.; Cheng, L.; Zhang, R.; Yang, Z. Impact of high-pressure homogenization on physico-chemical, structural, and rheological properties of quinoa protein isolates. *Food Struct.* **2022**, *32*, 100265. [CrossRef]

64. Ooi, Z.-Y.; Othman, N.; Choo, C.-L. The Role of Internal Droplet Size on Emulsion Stability and the Extraction Performance of Kraft Lignin Removal from Pulping Wastewater in Emulsion Liquid Membrane Process. *J. Dispers. Sci. Technol.* **2015**, *37*, 544–554. [CrossRef]

65. Krebs, T.; Schroën, C.; Boom, R. Coalescence kinetics of oil-in-water emulsions studied with microfluidics. *Fuel* **2013**, *106*, 327–334. [CrossRef]

66. Rogers, J.R.; Davis, R.H. Modeling of collision and coalescence of droplets during microgravity processing of Zn-Bi immiscible alloys. *Met. Mater. Trans. A* **1990**, *21*, 59–68. [CrossRef]

67. de Folter, J.W.J.; van Ruijven, M.W.M.; Velikov, K.P. Oil-in-water Pickering emulsions stabilized by colloidal particles from the water-insoluble protein zein. *Soft Matter* **2012**, *8*, 6807–6815. [CrossRef]

68. Tcholakova, S.; Denkov, N.D.; Sidzhakova, D.; Campbell, B. Effect of Thermal Treatment, Ionic Strength, and pH on the Short-Term and Long-Term Coalescence Stability of β-Lactoglobulin Emulsions. *Langmuir* **2006**, *22*, 6042–6052. [CrossRef] [PubMed]

69. Zhong, Y.; Xiang, X.; Wang, X.; Zhang, Y.; Hu, M.; Chen, T.; Liu, C. Fabrication and characterization of oil-in-water emulsions stabilized by macadamia protein isolate/chitosan hydrochloride composite polymers. *Food Hydrocoll.* **2020**, *103*, 105655. [CrossRef]

70. Yang, Z.; de Campo, L.; Gilbert, E.P.; Knott, R.; Cheng, L.; Storer, B.; Lin, X.; Luo, L.; Patole, S.; Hemar, Y. Effect of NaCl and CaCl2 concentration on the rheological and structural characteristics of thermally-induced quinoa protein gels. *Food Hydrocoll.* **2021**, *124*, 107350. [CrossRef]

71. Araiza-Calahorra, A.; Sarkar, A. Pickering emulsion stabilized by protein nanogel particles for delivery of curcumin: Effects of pH and ionic strength on curcumin retention. *Food Struct.* **2019**, *21*, 100113. [CrossRef]

72. Gould, J.; Vieira, J.; Wolf, B. Cocoa particles for food emulsion stabilisation. *Food Funct.* **2013**, *4*, 1369–1375. [CrossRef]

73. Kurukji, D.; Pichot, R.; Spyropoulos, F.; Norton, I. Interfacial behaviour of sodium stearoyllactylate (SSL) as an oil-in-water pickering emulsion stabiliser. *J. Colloid Interface Sci.* **2013**, *409*, 88–97. [CrossRef]

74. Chang, C.; Tu, S.; Ghosh, S.; Nickerson, M. Effect of pH on the inter-relationships between the physicochemical, interfacial and emulsifying properties for pea, soy, lentil and canola protein isolates. *Food Res. Int.* **2015**, *77*, 360–367. [CrossRef]

75. Liang, H.-N.; Tang, C.-H. pH-dependent emulsifying properties of pea [*Pisum sativum* (L.)] proteins. *Food Hydrocoll.* **2013**, *33*, 309–319. [CrossRef]

76. Sharif, H.R.; Williams, P.A.; Sharif, M.K.; Abbas, S.; Majeed, H.; Masamba, K.G.; Safdar, W.; Zhong, F. Current progress in the utilization of native and modified legume proteins as emulsifiers and encapsulants—A review. *Food Hydrocoll.* **2018**, *76*, 2–16. [CrossRef]